ELSEVIER

Journal of Organometallic Chemistry 544 (1997) 55–63

Journal of Organometallic Chemistry

Redox responsive bi/tri-nuclear complexes incorporating ferrocenyl unit: Synthesis, characterization, physicochemical studies and X-ray structure of $[C_5H_5FeC_5H_4CH=CHC_5H_4N\text{–}CH_3]PF_6$ with a mirror creating disorder

Amitava Das *, H.C. Bajaj [1], M.M. Bhadbhade

Central salt and Marine Chemicals Research Institute, Bhavnagar 364002, India

Received 6 March 1997

Abstract

(*Trans*-1-(4-pyridyl)–ethylene) ferrocene, L reacts with K[Ru^{III}(edtaH)]Cl to form binuclear complex. K[Ru^{III}(edtaH)]Cl exist as Ru^{III}(edtaH)(H_2O) in aqueous solution and substitution of the aqua molecule by L occurs within the stopped flow time scale. Rate constants for the reaction are 1620 ± 20, 2080 ± 35, 2690 ± 50 M^{-1} s^{-1} at 28, 34 and 39.9°C, respectively [$\Delta H^{\#}$ is 30.3 ± 1.1 kJ mol^{-1} and $\Delta S^{\#}$ is -124 ± 4 J K^{-1} mol^{-1}]. R^{II}(2,2′-bipy)$_2Cl_2$ reacts with L to form bi/trinuclear complexes, [Ru^{II}(2,2′-bipy)$_2$LCl]PF_6 and [Ru^{II}(2,2′-bipy)$_2L_2$]$(PF_6)_2$, depending on the reaction conditions. Luminescence of the Ru^{II}(2,2′-bipy)$_2$(py)$_2^{2+}$ center in the trinuclear complexes is completely quenched presumably through energy transfer pathway. There exist a moderate to weak electrochemical interaction between the two redox centers either in *N*-methylated form of L or in the bi/trinuclear complexes derived from Ru(II) or Ru(III). All these new bi/trinuclear complexes are characterized by physicochemical methods. Single crystal X-ray structure of $[L\text{–}CH_3]PF_6$ is reported. A very low value of powder SHG efficiency observed earlier for this salt can now be well understood in terms of the centrosymmetric molecular arrangement created due to the disorder in the crystal. © 1997 Elsevier Science S.A.

Keywords: Synthesis; Polynuclear complexes; Ferrocene; Physicochemical studies; Kinetics; X-ray structure

1. Introduction

The study of polynuclear metal complexes in which the redox and/or photoactive metal centers are electronically coupled through an unsaturated bridging ligand is of considerable current interest owing to the rapid growth of material science [1–4]. Specific emphasis has been placed on the designing and development of multinuclear assemblies capable of intermetallic energy- or electron-transfer processes [5–12]. In this regard ferrocene based molecules are currently attracting a great deal of attention owing to its unique redox behavior, remarkable stability and easy derivatisation of the ferrocene unit [13–29]. Metallocenes and in particular ferrocene containing molecules are becoming increasingly significant in designing (a) molecular sensor [1–4,30–34], (b) molecular ferromagnets [35,36], (c) electrochemical agents [37], (d) molecular switches [38,39], (e) liquid crystalline material [40,41] and (f) NLO materials [1–3,42–45]. A number of ferrocene derivatives are now known to exhibit a high degree of second order polarization effect; where the ferrocenyl moiety act as the donor of a donor–π–acceptor system [42–45].

As a part of our continued interest in the field of redox responsive donor–acceptor type polynuclear systems, we wish to report herein synthesis, characterization and physicochemical studies of bi/tri-redox system (Fig. 1) based on the pyridyl derivative of ferrocene. [Ru(edtaH)(H_2O)] is known to react with pyridine or substituted pyridine to form the corresponding pyridyl derivatives through a facile aqua substitution path [46,47]. We have utilized this reaction to synthesize a new mixed-valence binuclear complex I, while L reacts with Ru(2,2′-bipy)$_2Cl_2$ to form the bi/tri-nuclear complex (II and III) through loss of one/two labile Cl^- ion(s). A single crystal X-ray structure of $[L\text{–}CH_3]PF_6$

* Corresponding author.
[1] Also corresponding author.

PII S0022-328X(97)00309-4

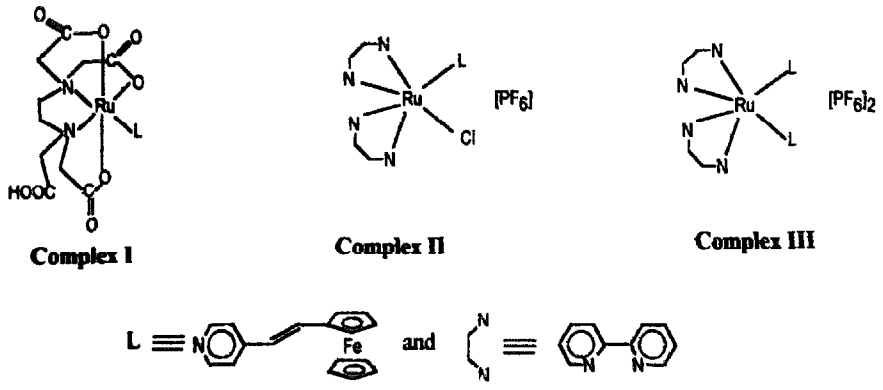

Fig. 1. Structure of the ligand, (*trans*-1-(4-pyridyl)ethylene)ferrocene and the complexes I–III.

is reported and a very low value of powder SHG efficiency observed earlier [29] is correlated with the molecular packing in the crystal, exhibiting mirror disorder.

2. Experimental

2.1. Materials

L[(*trans*-1-(4-pyridyl)ethylene))ferrocene], Ru(2,2'-bipyridyl)$_2$Cl$_2$.H$_2$O and K[Ru(edta)Cl]2H$_2$O were prepared following the known methods [22,46–48]. LDA was produced in situ by reacting an equimolar amount of *n*-butyllithium and di-isopropyl amine in dry THF. Ferrocene carboxaldehyde and *n*-butyl lithium were used as received from Aldrich. Di-isopropyl amine (National Chemicals, India) and pyridine were dried and distilled over CaH$_2$ before use. POCl$_3$ was used as received from Spectrochem (India). Bu_4NPF_6 and Bu_4NClO_4 were used as background electrolyte for electrochemical studies. Acetonitrile, used as solvent in electrochemical analysis was dried and distilled before use. Water used was doubly distilled. All reactions were performed under argon atmosphere.

2.2. Physical measurements

Microanalysis (C, H, N) were performed using a Perkin–Elmer elemental analyzer. IR-spectra were recorded as KBr pellets on a Carl–Zeiss Specord M80. Electronic spectra were recorded on a Shimadzu UV-3100 PC spectrometer. Fluorescence measurement was done on a Perkin–Elmer LS 50B luminescence spectrophotometer. EPR studies were carried out on a Bruker ESP 300 X spectrometer either at room temperature or at 77 K using a Dewar insert in the sample chamber and spectra were calibrated with DPPH (g = 2.0037). ^{1}H NMR spectra were recorded either on a JEOL 100 or Bruker GX 400 spectrometer. Fast-atom bombardment measurement were carried out on VG-ZAB instruments. Electrochemical experiments were performed by using a Princeton Applied Research (PAR 174A) electrochemical instrument. A conventional three-electrode cell assembly was used. A saturated calomel electrode as reference and platinum as working electrode were used for this purpose. For CV studies in non-aqueous solvent ferrocene was added at the end of each experiment as an internal standard. pH measurements were carried out with a Digisun pH meter.

2.3. Kinetic studies

The kinetics of the substitution of an aqua molecule in [Ru(edta)(H$_2$O)]$^-$ with L was studied spectrophotometrically (at 570 nm), using HI-Tech stopped-flow spectrophotometer coupled with an Apple IIe data analyzer. Pseudo first order condition (excess L) was used for all the kinetic runs and the corresponding first order plots were linear for at least 3–4 half lives of the reaction. Rate constant data presented, are the average of the at least 3–5 individual kinetic runs and are reproducible within ±5%. Acetic acid–acetate buffer was used to maintain the pH of the kinetic solution and KCl was used to control the ionic strength of the reaction medium. All kinetic runs were performed in 3:7 (v/v) methanol–water mixed solvent media.

2.4. Synthesis

2.4.1. N-Methylation of L

N-Methylation of L achieved a 85% yield by reaction of L (100 mg, 0.35 mmol) with a large excess of methyl iodide (1 ml) in CH_2Cl_2 under reflux for 18 h. The mixture was then evaporated and redissolved in a minimum volume of CH_3OH, to which excess NH_4PF_6 was added and stirred for 5 min at room temperature; [L–Me]PF_6 precipitated on cooling. It was filtered and recrystallized from CH_3OH. X-ray quality crystal was obtained by diffusion of ether vapor in the methylene chloride solution of [L–Me]PF_6. ^{1}H NMR (100 MHz), CD_3CN, δ (ppm): 4.12 (3H, s, NCH_3); 4.23 (5H, s,

cp); 4.60 (2H, br, cp' H^3/H^4; 4.71 (2H, br, cp', H^2/H^5); 6.86 (1H, d, $J = 16$ Hz, HC = CH); 7.76 (1H, d, $J = 16$ Hz, HC = CH); 7.83 (2H, d, $J = 4.2$ Hz, py H^3/H^5); 8.33 (2H, d, $J = 4.2$ Hz, py H^2/H^6). Anal. calculated for $FeC_{18}H_{18}PN\ F_6$: C 48.1, H 4.1, N 3.1; Found C 48.0, H 4.1, N 3.0.

2.4.2. *[Ru(edtaH)L], [I]*

150 mg (0.3 mmol) of K[Ru(edtaH)]Cl was dissolved in a minimum volume of dd water to which L (130 mg, 0.45 mmol) dissolved in 10 ml (1:1 v/v ethanol and water) was added (color of the solution changes from red to violet) and stirred for 15 min at room temperature under argon atmosphere. Then ethanol was removed under reduced pressure and excess L was removed by solvent extraction in CH_2Cl_2 layer. The aqueous solution was then concentrated to 2 ml under reduced pressure. The desired compound was precipitated by addition of excess methanol, filtered and washed thoroughly with aqueous–acetone (2:8, v/v) mixture. Then the solid was further crystallized from water and cold methanol (yield: 180 mg; 85%). Anal. calculated for $RuFeC_{27}H_{28}N_3O_8.2H_2O$: C 45.3, H 4.5, N 5.9; Found C 45.1, H 4.5, N 5.9.

2.4.3. *[Ru(2,2'-bipy)$_2$(L)Cl)]PF$_6$, [II]*

$Ru(2,2'\text{-bipy})_2Cl_2$ (150 mg, 0.29 mmol) and L (125 mg, 0.43 mmol) was refluxed in 50 ml of ethanol–water mixture for 8 h under argon. Then volume was reduced to ~ 10 ml under reduced pressure. To which a saturated solution of KPF_6 was added with stirring. The desired compound was precipitated and filtered off. The residue was washed with cold water, dried and purified by column chromatography on silica (60–120 mesh) using CH_3CN — saturated aqueous solution of KPF_6 and water (97:2:1 v/v) as eluent. The major reddish brown fraction was collected and dried by rota-evaporation. Excess KPF_6 was removed in water layer by solvent extraction with methylene chloride. CH_2Cl_2 layer containing the desired complex was dried over $MgSO_4$ and evaporated to dryness (Yield: 50 mg, 21%). FAB Mass: $M/Z = 883$, (M^+), 738, (M^+-PF_6). ^1H NMR (100 MHz) (CD_3CN): 4.12 (5H, s, cp), 4.40 (2H, s, cp', H^3/H^5), 4.56 (2H, s, cp', H^2/H^6), 6.58 (1H, $J = 16$ Hz, d, 1HC = CH), 7.1–8.9 (23H, m, $py^{3,5}$, 2,2'-bipy, 1HC = CH), 8.98 (2H, d, $J = 4.2$ Hz, $pyH^{2,6}$) Anal. calculated for $RuFeC_{37}H_{31}N_5PClF_6$.: C 41.5, H 4.1, N 9.3; Found C 41.7, H 4.3, N 9.1.

2.4.4. *[Ru(2,2'-bipy)$_2$(L)$_2$](PF$_6$)$_2$, [III]*

Its synthetic procedure is almost similar to that for complex II. In this case L was used in large excess (420 mg, 1.44 mmol) and was refluxed for 4 h in 15 ml of ethylene glycol medium. The desired product was purified by column chromatography (yield: 120 mg, 34%). Along with this little amount of complex II (< 5%) was obtained.: FAB Mass (M/Z): 1283(M^+), 1134(M^+-PF_6), 991(M^+-2PF_6). ^1H NMR (400 Mhz, CD_3CN): 4.13 (10H, s, cp), 4.42 (4H, t, $J = 1.9$ Hz, cp'), 4.51 (4Hi, t, $J = 1.9$ Hz, Cp'), 6.66 (2H, d, $J = 16$ Hz, 2 HC = CH), 7.2–8.2 (22H, m, 2,2'-bipy, 2HC = CH), 8.36 (2H, d, $J = 4.2$ Hz, $pyH^{3,5}$), 8.98 (2H, d, $J = 4.2$ Hz, pyH). Anal. calculated for $RuFe_2C_{54}H_{38}N_6P_2F_{12}$: C 50.6, H 3.6, N 6.6; Found C 51.0, H 3.7, N 63.

2.5. Crystal structure determination

Crystallographic details of $[L\text{–}CH_3]PF_6$ are summarized in Table 1. Preliminary data and systematic absences indicated that the compound belong to the monoclinic space-group $P2_1$ or $P2_1/m$. Since the molecule as such does not possess a plane of symmetry and the cell

Table 1
Crystal data and structure refinement for $[C_5H_5FeC_5H_4CH=CHC_5H_4N\text{–}CH_3]PF_6$

Crystal data	
$FeC_{18}H_{18}PNF_6$	MoK_α radiation
$Mr = 392.15$	$\lambda = 0.71073$ Å
Monoclinic $P2_1/m$	Cell parameters from 25 reflections
$a = 7.068(6)$ Å	$\theta = 8–14°$
$b = 9.297(4)$ Å	$\mu = 0.96$ mm^{-1}
$c = 13.661(4)$ Å	$T = 295$ K
$\beta = 92.00(5)°$	Needles 0.30 × 0.08 × 0.06 mm
$V = 897.1(9)$ Å^3	Dark red brown
$Z = 2$	
$D_x = 1.452$ g cm^{-3}	
Data collection	
Enraf–Nonius CAD-4 diffractometer	1160 observed reflection
$\omega/2\theta$ scan	$[I > 2\sigma(I)]$
1269 measured reflection	$\theta_{max} = 22.5°$
1269 independent reflections	$h = -7 \rightarrow 7$
3 Standard reflections, frequency: 60 min.	$k = 0 \rightarrow 10$
intensity decay < 1%	$l = 0 \rightarrow 14$
Refinement	
Refinement on F_0^2	$w = 1/[\sigma^2(F_0^2) + (0.1200P)^2 + 3.3500P]$
$R = 0.067$	$p = (F_0^2 + 2F_c^2)/3$
$wR = 0.223$	$(\Delta/\sigma)_{max} = 0.2$
$S = 1.259$	$\Delta\rho_{max} = 1.17$ e Å^{-3}
1269 reflections	$\Delta\rho_{min} = -0.38$ e Å^{-3}
132 parameters	Atomic scattering factors from international table for X-ray crystallography (1974, vol. IV)
H-atom parameters refined as in riding model	

Data collection: CAD-4 Software (CAD-4 software, Version 5, Enraf–Nonius, Delft). Cell refinement: CAD-4 Software. Data reduction: NRCVAX [49].

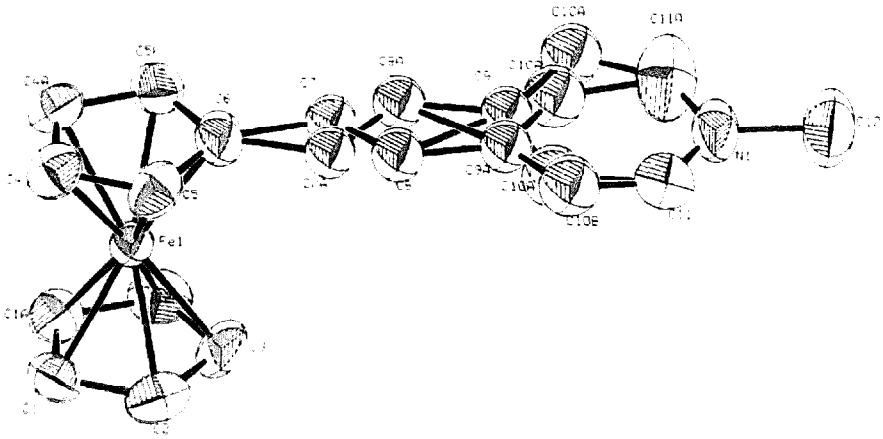

Fig. 2. ORTEP view of the complex cation $[C_5H_5FeC_5H_4CH=CHC_5H_4N\text{–}CH_3]PF_6$, ellipsoids are plotted at the 50% probability level.

volume accommodated only two formula units, the choice of the non-centrosymmetric space group was preferred, which later turned out to be incorrect. The structure was solved using the program SHELX-86 [50] by heavy-atom method. The progress of the structure solution and refinement revealed the correct space group to be $P2_1/m$ with the complex cation and the PF_6^- anion occupying a special position (mirror–plane) in the unit cell. As for the octahedral PF_6^-, the mirror symmetry can easily be visualized; in case of the complex cation, the ethylene linkage which breaks this symmetry acquires it 'statistically' by distributing the double bond over the two mirror related positions. The anisotropic full-matrix least-squares refinement of all the non-hydrogen atoms (except for the disordered atoms C7 and C8 which were refined isotopically) using the program SHELXL-93 [51] revealed large anisotropy for the atoms C9 and C10. These atoms were split into two positions each with half-occupancy, as suggested by the program on the basis of a very high U22 component (Fig. 2). Further cycles of least-squares with the disordered positions of C9 and C10 treated isotopically resulted in a marked improvement in the refinement parameters and more reasonable geometrical parameters involving these atoms. It is noteworthy that the atom C6 of the ferrocene moiety attached to the other end of the double bond does not show any such effect. Anisotropy of the rest of the atom in the py–CH_3 unit are large, but not as much to consider the alternative sites for them. This model of disorder with the rigid ferrocene moiety to be perfectly ordered and the only pendant arm having two alternative positions in the unit cell seems very reasonable and the refinement results (Table 1) endorse it. Final cycles of full-matrix least-squares were carried out including the calculated positions of the H-atoms with appropriate occupancies. The final positional parameters of non-hydrogen atoms are given in Table 2.

Table 2
Atomic coordinates ($\times 10^4$) and equivalent isotropic displacement parameters ($Å^2 \times 10^3$) for $[L\text{–}CH_3]PF_6$. U_{eq} is defined as one third of the trace of the orthogonalized U_{ij} tensor

	X	Y	Z	U_{eq}
Fe(1)	2236(2)	2500	34(1)	38(1)
C(1)	2093(10)	1747(9)	−1386(5)	51(2)
C(2)	3782(11)	1274(9)	−877(6)	60(2)
C(3)	4834(14)	2500	−585(9)	60(3)
C(4)	−96(10)	1739(8)	705(5)	51(2)
C(5)	1546(10)	1269(9)	1203(5)	54(2)
C(6)	2575(15)	2500	1531(7)	56(3)
C(7)	4377(18)	2893(13)	2093(9)	45(4)
C(8)	5410(20)	1868(16)	2502(10)	49(3)
C(9)	7192(20)	2908(14)	3027(10)	47(4)
C(10A)	8039(29)	1539(26)	3188(15)	67(5)
C(10B)	8152(27)	922(25)	3428(14)	66(5)
N(1)	10639(13)	2500	4043(7)	70(3)
C(11)	9805(14)	1255(13)	3802(7)	88(3)
C(12)	12466(18)	2500	4624(11)	99(6)
P(1)	6992(4)	2500	−3537(2)	52(1)
F(1)	7394(11)	1315(9)	−2774(6)	137(3)
F(2)	6572(12)	1349(10)	−4370(6)	151(3)
F(3)	4863(12)	2500	−3311(7)	119(4)
F(4)	9140(12)	2500	−3771(8)	128(4)

3. Results and discussion

3.1. Protonation constant

Protonation constant, pK, for the appended pyridine group in L was determined by spectrophotometric titration in mixed solvent (water/alcohol; 1:1; v/v) at 25°C and $\mu = 0.1$ M Bu_4NClO_4. pK was obtained from a plot of the ratio of absorbance at 313 nm (λ_{max} for the unprotonated form of L) and 358 nm (λ_{max} for the protonated form of L) versus pH (Fig. 3). pK for L (5.2) is lower compared to free pyridine or 4,4'-bipyridyl-1,2-ethylene (5.9) [52]. It signifies the moderately strong back-bonding involving Fe and the substituted cp ring.

3.1.1. Synthesis

The K[Ru(edtaH)Cl] · $2H_2O$ complex is rapidly equated when dissolved in water to give Ru(edtaH)(H_2O) [52–54], which undergo a facile aqua substitution reaction with aromatic *n*-heterocycles [53,55,56]. We have utilized this reaction to synthesize the respective binuclear complex, Ru(edtaH)(L). Reaction of K[Ru(edtaH)Cl] with 2 equivalents of L in water–CH_3OH mixed solvent resulted in formation of reddish–violet binuclear complex I. Results of the elemental analysis are in good agreement with the proposed formulation. IR spectra of complex I exhibited stretching bands at 1715, 1680, 1630 and 1600 cm^{-1}. Bands at 1715 and 1680 cm^{-1} are assigned to coordinated –COO and uncoordinated –COOH respectively [55–58]. Bands at 1630 and 1600 cm^{-1} were due to the presence of a ferrocenyl moiety [59]. [Ru(2,2′-bipy)$_2$ · Cl_2]$2H_2O$ reacts with L to form either complex II or III depending on the reaction condition. Reaction at lower temperature with slight molar excess of L yield complex II relatively better while during the reaction at higher boiling solvent (ethylene glycol) and higher ratio (5 times) of molar equivalence of L, complex III is formed preferentially. Elemental analysis data for complex II and III are in good agreement with the proposed formulation. ^1H NMR spectra for [L–CH_3]PF_6, complex II and III are also in excellent agreement with the proposed formulation. In particular the ^1H NMR spectra of [L–CH_3]PF_6, complex II and III indicate that only the less hindered E isomers have formed (J = 16 Hz for the *trans* pair of protons on the ethylene double bond). In case of the *N*-methylated form of L this has been confirmed by structural analysis. We can presume that complex I also exist in E form [50,59,60].

3.2. X-ray crystallography

An ORTEP [61] view of the complex cation, [L–CH_3]$^+$ with the atom numbering is shown in Fig. 2. As discussed earlier, the molecule possesses only a statistical mirror plane because of the two-fold disorder of the pendant arm. Had this disorder not been present, the crystal would belong to the non-symmetric space group $P2_1$, an essential criterion for observing a SHG (second harmonic generation) efficiency [29]. A very low value (almost zero) of powder SHG efficiency observed for this salt [29] can now be well understood in terms of the centrosymmetric molecular arrangement created due to the disorder in the crystal. From the crystallographic details reported for the NO_3^- salt, it is likely that even the crystal structure of this salt [29] may contain the same disorder. An unusually short C = C ethylene bond distance, maximum residual electron densities observed at the ethylene carbons, slow progress of the least-squares refinement, etc. could all be indicators of this behavior. Of course, the extent of the disorder may not be a 50:50% as the mirror symmetry demands in the present structure, but there could be a partial disorder of the ethylene carbon atoms [22]. Reduced SHG efficiency of this salt could then be correlated with the symmetric contribution that would arise from such a disorder. Selected bond distances and angles given in Table 3 are in good agreement with the reported values and the geometry involving the disordered atoms devi-

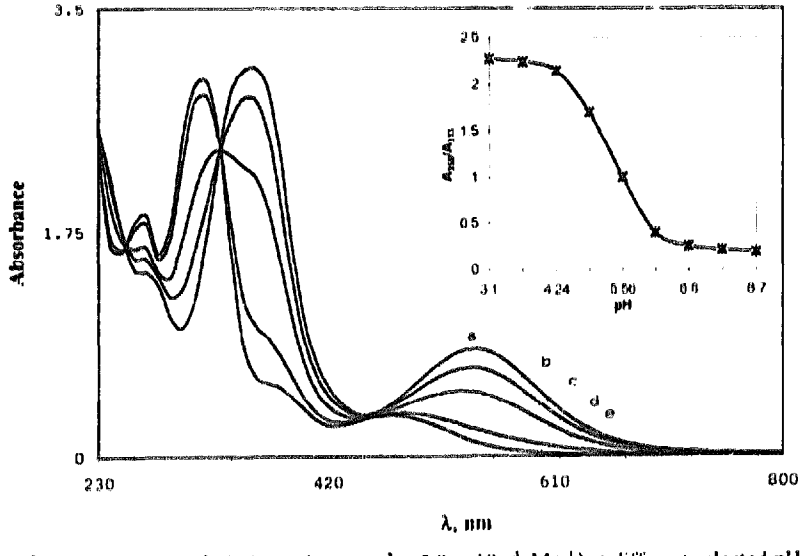

Fig. 3. UV-visible spectra of L, [*trans*-1-(4-pyridyl)ethylene-ferrocene] = 5.0×10^{-4} M^{-1}) at different selected pH (for the sake of clarity in 1:1 water–alcohol mixture pH = (a) 3.10, (b) 4.24, (c) 5.56, (d) 6.80, (e) 8.70; Inset: plot of the ratio of absorbance at 313 nm (λ_{max} for the unprotonated form of L) and 358 nm (λ_{max} for the protonated form of L) versus pH.

Table 3
Selected bond lengths (A) and angles (deg) for $[L\text{-}CH_3]PF_6$

Fe(1)–C(1)	2.062(7)	Fe(1)–C(2)	2.034(8)
Fe(1)–C(3)	2.048(10)	Fe(1)–C(4)	2.040(7)
Fe(1)–C(5)	2.038(7)	Fe(1)–C(6)	2.051(10)
C(1)–C(2)	1.429(11)	C(2)–C(3)	1.411(11)
C(5)–C(4)	395(11)	C(5)–C(6)	1.421(10)
C(6)–C(7)	1.51(2)	C(7)–C(8)	1.31(2)
C(8)–C(9)	1.72(2)	C(9)–C(10B) [a]	1.39(3)
C(10A)–C(11)	1.50(2)	C(10B)–C(11)	1.30(2)
N(1)–C(11)	1.335(12)	N(1)–C(12)	1.49(2)
P(1)–F(1)	1.536(7)	P(1)–F(2)	1.582(7)
P(1)–F(3)	1.547(9)	P(1)–F(4)	1.562(9)
C(5)–C(6)–C(5) [a]	107.4(9)	C(5) [a]–C(6)–C(7)	112.3(6)
C(7)–C(8)–C(9)	99.1(11)	C(8)–C(7)–C(6)	119.2(10)
C(10B) [a]–C(9)–C(10B)	117(2)	C(11)–C(10B)–C(9) [a]	113(2)
C(10B)–C(11)–N(1)	133.5(14)	C(11)–N(1)–C(12)	119.9(6)
N(1)–C(11)–C(10A)	109.7(13)	F(1) [a]–P(1)–F(1)	91.7(7)
F(1)–P(1)–F(2)	91.6(5)	F(1)–P(1)–F(3)	91.3(4)
F(1)–P(1)–F(4)	88.9(4)	F(3)–P(1)–F(4)	179.7(6)
F(3)–P(1)–F(2)	89.1(4)	F(4)–P(1)–F(2)	90.7(5)

Symmetry transformations used to generate equivalent atoms: [a] $x, -y+1/2, z$.

ate from the normal expected values. The side arm (in both the orientations) is nearly coplanar with the cyclopentadienyl ring to which it is attached, thus having a considerable π-electron overlap over the entire moiety.

3.3. Kinetic study

Spectral change i.e. increase in absorbance at 525 nm associated with the formation of complex I was used to study the kinetics of the substitution reaction (Eq. (1)). $Ru(edta)(H_2O)^-$ is known to show maximum reactivity [52–54,57] in pH range 4–6. Thus kinetics of the reaction was studied at pH 6.0 (acetic acid–acetate buffer) under pseudo first order conditions (excess

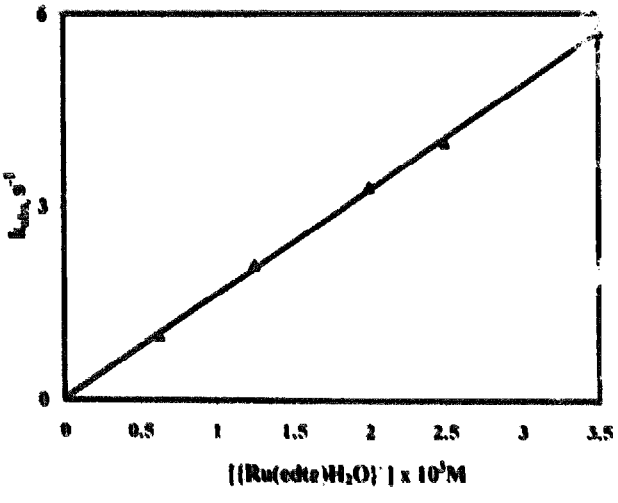

Fig. 4. Plot of k_{obs} versus $[Ru(edta)(H_2O)^-]$ at $T = 25 \pm 0.1$°C, pH = 6.0 (acetic acid/acetate buffer) $\mu = 0.5$ M (KCl). [L], *trans*-1-(4-pyridyl)ethylene ferrocene = 5.0×10^{-4} M.

$Ru(edta)(H_2O)^-$) and at this pH, L exists predominantly (> 90%) in the unprotonated form (vide supra). Moreover, the minor protonated form is expected to be unreactive. The rate of reaction was found to be first order with respect to [L] and $[Ru(edta)(H_2O)^-]$. k_{obs} increases with the increase in $[Ru(edta)(H_2O)]^-$ (Fig. 4). A small intercept for the k_{obs} versus $[Ru(edta)(H_2O)^-]$ plot indicates the slow reverse aqueous reaction under the specified condition [57,58]. k_f and k_r for this substitution reaction (Eq. (1)) at 28°C and $\mu = 0.5$ M (KCl) are 1620 ± 20 M^{-1} s^{-1} and $(1.8 \pm 10.2) \times 10^{-2}$ s^{-1} (log K = 4.96). Moreover, reaction rates remain unchanged when a few runs were repeated in inert (Argon) atmosphere. Reaction rates are also independent of ionic strength and remain unchanged over a concentration range of 0.1 to 0.5 M of KCl. Based on the above kinetic observations, the following mechanism (Eq. (1)) and rate law (Eq. (2)) is proposed for the formation of complex I. The substitution reaction was studied at three different temperatures and values of the rate constants are 1620 ± 20, 2080 ± 35, 2690 ± 50 M^{-1} s^{-1} at 28, 34 and 39.9°C respectively. Small $\Delta H^{\#}$ value (30.3 ± 1.1 kJ mol^{-1}) and large negative $\Delta S^{\#}$ (-124 ± 4 J K^{-1} mol^{-1}) are consistent with the associative mechanism [52–54,58].

$$Ru(edta)(H_2O)^- + L \underset{k_r}{\overset{k_f}{\rightleftharpoons}} Ru(edta)L^- + H_2O \qquad (1)$$

$$k_{obs} = k_f[L] + k_r \qquad (2)$$

3.4. Electrochemical analysis

Electrochemical results are summarized in Table 4. The ferrocene derivative is known to undergo reversible

Table 4
Electrochemical data [a]

Complexes	$E_{1/2}$ (Fc/Fc$^+$)/ V (ΔE/mV)	$E_{1/2}$ ($Ru^{II/III}$)/ V (ΔE/mV)	$E_{1/2}$ (N^+–Me/N–Me)/ V (ΔE/mV)	$E_{1/2}$ (Ligand based, bp/bp$^-$)/ V (ΔE/mV)
L	0.44	—	—	—
Ru(edtaH)py	—	−0.15 (90) [b]		
[L–Me]PF_6	0.55 (70)	—	1.25 (90)	—
Complex I [b]	0.52 (80)	−0.18 (110) [c]	—	—
Complex II	0.49 (70)	0.74 (75)	—	1.53 (100), −1.74 (120)
Complex III	0.50 (85)	1.28 (120)	—	1.54 (110), −1.73 (130)

[a] CV studies were performed in CH_3CN media unless mentioned otherwise.
[b] Experiments were performed in H_2O, see also Refs. [55,56].
[c] Quasireversible process. $E_{1/2}$ quoted for the scan rate of 200 mV/s versus SCE as reference electrode.

one electron oxidation at slightly more anodic potential compared to unsubstituted ferrocene [22,62] and can be attributed to the linkage to pyridyl unit through conjugation. All binuclear complexes (I–III) and [L–Me]PF_6 undergo two distinct one electron redox processes. Comparison of $E_{1/2}$ values for L and *N*-methylated analogue gives a good indication of effective electronic interactions between the two redox active ends. *N*-methylation of the pendant pyridyl group causes a anodic shift in the $E_{1/2}$ value for the Fc/Fc$^+$ couple with respect to that of free ferrocene. The extent of the anodic shift is similar to that observed for the *N*-methylated derivative of the molybdenum polypyrazolylborate system where the two redox centers are separated by similar distance through a conjugated spacer and also the metal orbital are known to have appreciable overlap with the ligand orbital [10,63]. The magnitude of electrochemical interaction, $\Delta E_{1/2}$, in binuclear or biredox systems may be evaluated by comparison with the redox potentials of mononuclear counterparts (Table 4). In case of complete cut off of the electronic communication, the $E_{1/2}$ values for the Fc/Fc$^+$ and $Ru^{III/II}$ couple are expected to remain unchanged, while an anodic shift of 80 mV for the Fc/Fc$^+$ couple and an cathodic shift of 30 mV are observed for the $Ru^{III/II}$ couple in complex I. Thus there exist a donor–acceptor type interaction. This interaction is 120 mV for the *N*-methylated product. The extent of electrochemical interaction is smaller for II (50 mV) and III (60 mV). In both cases the $E_{1/2}$ value for the $Ru^{II/III}$ couple is almost invariant. Similar small electrochemical interaction has been observed for other binuclear complexes derived from substituted Ru(2,2′-bipy)$_3^{2+}$ or Ru(terpy)$_2^{2+}$ [18,59,64]. For Ru(2,2′-bipy)$_2$(py)$_2^{2+}$ (py = pyridine or substituted pyridine) there always exist a competition between $d\pi_{Ru} \rightarrow \pi^*_{bpy}$ and $d\pi_{Ru} \rightarrow \pi^*_{py}$ for back bonding and in most instances back bonding involving the π^* orbital of bipyridyl are most important, leaving the d_π orbital of Ru(II) less available to interact with the π^* orbital of pyridine [65]; while, in case of the Ru(edta)-system, the Ru(III) center is reported to have a weak π donating ability. Presumably this accounts for the low electrochemical interaction between the ruthenium center and the ferrocene moiety. Similar moderate to weak electrochemical interaction was reported for binuclear complexes derived from covalently linked ferrocene [59]. However, higher electrochemical interaction was observed [66,67] for the Ru(2,2′-bipy)$_2$(CN)$_2$Cr(CN)$_5$ complex. Presumably the longer distance of separation between the metal centers in II and III accounts for the lower interaction. Reduction observed at ~ -1.5 V and ~ -1.7 V for complexes II and III are due to the two co-ordinated bipyridyl units.

3.5. Epr spectroscopy

Apart from complex I all other complexes are diamagnetic. EPR spectral pattern of complex I, both in powder and frozen solution (77 K; H_2O–DMSO/30:70(v/v)) is almost similar [55,56] to that for Ru(edta)(py)$^-$ and characteristic g values were observed, as reported for other complexes of Ru–edta with π-acid ligands [55,56,68]. As the Fe(II) center is diamagnetic, the Ru(III)-center is magnetically isolated and no magnetic exchange interaction with the iron center is possible and also there is no marked rearrangement in geometry of the Ru–edta-center in complex I. No ruthenium hyperfine splitting was observed. Features observed at 2.52, 2.32 and 1.93 are assigned for g_1, g_2 and g_3 respectively.

3.6. UV-visible and Luminescence studies

UV-visible spectral data for all the complexes are given in Table 5. Unsubstituted ferrocene exhibit two weak bands at 325 and 440 nm, which has been assigned to the $^1A_{2g} \rightarrow {}^1E_{2g}$ and $^1A_{1g} \rightarrow {}^1E_{1g}$ ligand field (d–d) transition [69]. Upon substitution at Cp with the conjugated acceptor group, L, as expected, the low lying π^* ligand orbital shifts to lower energy (373 and 466 nm) and there is a increased mixing of ligand orbital and metal d-orbitals and thus d–d transition has become more allowed ($\varepsilon_{466} = 2800$ dm^3 mol^{-1} cm^{-1} for both transitions compared to ~ 50 for ferrocene)

Table 5
Electronic spectral data λ_{max} (nm) for the complexes

Complex	λ_{max},nm (ε, M^{-1} cm^{-1})
LH^{+} [a]	543 (5150), 358 (18700), 266 (8854)
[L–Me](PF_6) [b]	549 (5310), 360 (27000), 271 (5350),
I [c]	1220 (28), 520 (sh), 344 (9600), 271 (6000)
II [b]	502 (sh), 459 (9615), 375 (11670), 322 (135000), 289 (31750)
III [b]	510 (sh), 470 (17440), 382 (34830), 326 (35740), 291 (59780)

[a] Spectra recorded in 1:1 water–ethanol (v/v) media.
[b] In acetonitrile.
[c] In water.

[22]. This lowest energy transition may be considered as MLCT transition with some d–d character. The second lowest energy transition is $\pi-\pi^*$ involving conjugated side group with some d–d character [22]. Both these transitions are appreciably red shifted either on protonation or on *N*-methylation. In Ru(edta)(py) type complexes, the Ru(III)-center is not known to have any characteristic absorbance in the visible region [55,56]. Thus the spectrum in visible region for complex I is basically dominated by the ferrocenyl unit. Attachment of the Ru(III) center, known to behave as a σ-acid group [57], to the pendant pyridyl group in L, resulted in a red shift of ca. 50 nm: the Ru(edta) substituent therefore act as electron accepting group, which also has been established by electrochemical studies. However in the UV region the spectra of the ferrocene unit is masked by the strong absorbance due to the ligand based $n-\pi^*$ transition in the Ru(edta) chromophore. For complex I, a mixed valence complex, a very broad and weak inter valence charge transfer band appears at 1220 nm ($\varepsilon = 28$ M^{-1} cm^{-1}). The absorbances in the visible region, for complex II and III, is dominated by the Ru(2,2′-bipy)$_2$(py)$_2$ chromophore. Ru(2,2′-bipy)$_2$(py)$_2^{2+}$ has a characteristic MLCT band in the visible region, position of which is sensitive to the presence of substituents on the pyridyl ligand. Very broad absorbance in the visible region for complex II and III is due to the overlapping of the absorbance of the Ru(2,2′-bipy)$_2$(py)$_2$ and ferrocenyl unit. Contribution to the absorbance for the ferrocenyl unit(s) is expected to shift to the lower energy upon co-ordination of the pyridyl unit. Thus for both these complexes, shoulders that appear at the lower energy side (> 500 nm) are due to co-ordinated ferrocenyl unit(s). For all bi/tri nuclear complexes, we note that the absorption spectra of ferrocenyl based fragments exhibit tails extending to 650 nm, which is even more prominent in the *N*-methylated form of L and in I (in these cases tails extends to ~ 775 nm). Thus in the polynuclear complexes the lowest lying excited states are expected to be centered on the ferrocenyl moiety and are also of a sufficient low energy that energy transfer quenching could be thermodynamically allowed [10,70,71]. L, its protonated form, I and [Ru(2,2′-bipy)$_2$PyCl]PF_6, all are known to be non-emissive, where as [Ru(2,2′-bipy)$_2$(py)$_2$]$^{2+}$ (py = pyridine or simple substituted pyridine) is known to exhibit luminescence [72–76]. Luminescence properties of II and III were studied at room temperature and both compounds were found to be non-emissive. Thus in III, luminescence of the [Ru(2,2′-bipy)$_2$(py)$_2$]$^{2+}$ core ($^3E_1$ state) is completely quenched. Electrochemical data revealed that reductive electron transfer quenching of the [Ru(2,2′-bipy)$_2$(py)$_2$]$^{2+}$ unit by the covalently linked ferrocenenyl unit is thermodynamically forbidden as it is very difficult to reduce the ferrocene core: there is no reduction peak observed for the ferrocene unit within the solvent cut off window (> -2.2 V). Moreover the intermolecular dynamic quenching studies using ferrocene as a quencher show that ferrocene can quench very efficiently the triplet state of many organic molecules and inorganic complexes [61,77,78]. At room temperature the charge separated species in III is destabilized by at least +1.2 eV, which more than cancels out the thermodynamic gradient for electron transfer [78]. Thus it is logical to conceive energy transfer as the most plausible pathway for luminescence quenching of the ruthenium center and it behaves as a normal triplet donor when the covalently linked quencher has low-energy triplet levels available.

Acknowledgements

This work is supported by DST, New Delhi, India. Authors are thankful to Professor P. Natarajan, for his encouragement and to C.D.R.I. Lucknow for recording the FAB mass and 400 MHz ^{1}H NMR spectra.

References

[1] D.W. Bruce D. O'Hare (Eds.), Inorganic Materials, Wiley, Chichester, 1992.
[2] I. Hawkins, R.A. Clark, C.E. Waunwrite, A.E. Underhill, Mol. Cryst. Liq. Cryst. 181 (1990) 209.
[3] I.R. Butler, Specialist Periodical Report — Organometallic Chemistry, Vol. 21, Ch. 14, E.W. Able (Ed.), Cambridge, 1992.
[4] N.J. Long, Angew. Chem. Int. Ed. Eng. 34 (1995) 21.
[5] E.C. Constable, Chem. Ind. (1994) 56.
[6] M.S. Wrighton, in: Fine Chemicals for Electronic Industry, P. Banfield (Ed.), Royal Society of Chemistry, London, 1986, pp. 53–69.
[7] D.A. Bradwell, F. Barigelletti, R.L. Cleary, L. Flamigni, M. Guardigli, J.C. Jeffery, M.D. Ward, Inorg. Chem., 34 (1995) 2438 and Refs. therein.
[8] A.J. Amoros, A.W.M.C. Thompson, J.P. Maher, M.D. Ward, J.A. McCleverty, Inorg. Chem. 34 (1995) 4828.
[9] K.S. Schanze, D. MacQueen, T.A.S. Perkin, L. Albana, Coord. Chem. Rev. 122 (1993) 63.

[10] A.J. Amoroso, A. Das, J.A. McCleverty, M.D. Ward, F. Barigelletti, L. Flagmini, Inorg. Chim. Acta 226 (1994) 171.
[11] A. Das, J.C. Jeffery, J.A. McCleverty, E. Schatz, M.D. Ward, Angew. Chem. Int. Ed. Eng. 32 (1992) 1515.
[12] A. Das, J.P. Maher, J.A. McCleverty, J.A. Navas Badiola, M.D. Ward, J. Chem. Soc. Dalton Trans (1993) 681.
[13] E.C. Constable, Angew. Chem. Int. Ed. Eng. 30 (1991) 407.
[14] R. Giasson, E.J. Lee, X. Zhao, M.S. Wrighton, J. Phys. Chem. 97 (1993) 2596.
[15] S.B. Wilkes, I.R. Butler, A.E. Underhill, A. Kobayashi, H. Kobayashi, J. Chem. Soc. Chem. Commun. (1994) 53.
[16] D.R. Crisope, K.M. Park, G.B. Schuster, J. Am. Chem. Soc. 111 (1989) 6195.
[17] W.-J. Wang, W.-T. Wong, K.-K. Cheung, J. Chem. Soc. Dalton Trans (1995) 1379.
[18] I.R. Butler, N. Burke, L.J. Hobson, H. Findenegg, Polyhedron 11 (1992) 2435.
[19] L.L. Liai, J.Y. Dong, J. Chem. Soc. Chem. Commun. (1994) 2347.
[20] A.S. A-El-Aziz, K.M. Epp, C.R. de Denus, G.F. Smith, Organometallics 13 (1994) 2299.
[21] O. Carugo, G.D. Santis, L. Fabbrizzi, M.L. Licchelli, A. Monichino, Inorg. Chem. 31 (1992) 765.
[22] M.M. Bhadbhade, A. Das, J.C. Jeffery, J.A. McCleverty, J.A. Navas Badiola, M.D. Ward, J. Chem. Soc. Dalton Trans (1995) 2769.
[23] Y. Wang, K.S. Schanze, Inorg. Chem. 33 (1994) 1354.
[24] B.J. Coe, C.J. Jones, J.A. McCleverty, D. Bloor, C.H. Cross, T.L. Axon, J. Chem. Soc. Dalton Trans (1994) 3427.
[25] E.C. Constable, A.M.W.C. Thompson, J. Chem. Soc. Dalton Trans (1994) 1409.
[26] E.C. Constable, R.M. Manez, A.W.M.C. Thompson, J.V. Walker, J. Chem. Soc. Dalton Trans (1994) 1585.
[27] R. Bosque, C. Lopez, J. Sales, X. Solan, M.F. Bardia, J. Chem. Soc. Dalton Trans (1994) 735.
[28] R. Bosque, M.F. Bardia, C. Lopez, J. Sales, J. Silver, X. Solan, J. Chem. Soc. Dalton Trans (1994) 747.
[29] S.R. Marder, J.W. Perry, R.G. Tiemann, Organometall. 10 (1991) 1896.
[30] F. Barigelletti, L. Flamigni, V. Balzani, J.P. Collin, J.-P. Sauvage, A. Sour, E.C. Constable, A.M.W.C. Thompson, J. Chem. Soc. Chem. Commun. (1993) 942.
[31] R.W. Wagner, P.A. Brown, T.E. Johnson, J.S. Lindsey, J. Chem. Soc. Chem. Commun. (1991) 1463.
[32] P.D. Beer, Chem. Soc. Rev. 14 (1989) 409.
[33] P.D. Beer, C. Blackburn, J.F. McAleer, H. Sikanyika, Inorg. Chem. 29 (1990) 378.
[34] A. Houlton, S.K. Ibrahim, J.R. Dilworth, J. Silver, J. Chem. Soc. Dalton Trans (1990) 2421.
[35] J.S. Miller, A.J. Epstein, W.M. Reiff, Chem. Rev. 88 (1988) 201.
[36] J.S. Miller, A.J. Epstein, Angew. Chem. Int. Ed. Eng. 33 (1994) 385.
[37] D. Nicot, R. Mathien, D. Montaazon, G.G. Lavigne, J.P.I. Majora, Inorg. Chem. 33 (1994) 434.
[38] J.C. Medina, I. Gay, Z. Chen, L. Echegoyen, G.W. Gokel, J. Am. Chem. Soc. 113 (1991) 365.
[39] G.D. Santis, L. Fabbrizzi, M. Licchelli, P. Pallavicini, Inorg. Chim. Acta 225 (1994) 239.
[40] A. Warner, W. Friedrichsen, J. Chem. Soc. Chem. Commun. (1994) 365.
[41] R. Deschenaux I. Kosztics, U. Scholten, D. Guillon, M. Ibhelhay, J. Mater. Chem. 4 (1994) 1351.
[42] M.C.B. Colbert, A.J. Edward, J. Lewis, N.J. Long, N.A. Page, D.G. Parker, P.R. Raithby, J. Chem. Soc. Dalton Trans. (1994) 2589.
[43] K.L. Kolt, D.A. Higgins, R.J. McMahon, R.M. Corn, J. Am. Chem. Soc. 115 (1993) 5342.
[44] B.J. Coe, C.J. Jones, J.A. McCleverty, D. Bloor, G. Cross, J. Organomet. Chem. 464 (1994) 225.
[45] Z. Yuan, N.J. Taylor, Y. Sun, T.B. Marder, J. Organomet. Chem. 449 (1993) 27.
[46] A.A. Diamantis, J.V. Dubrawski, Inorg. Chem. 20 (1981) 1142.
[47] H.C. Bajaj, R. Van Eldik, Inorg. Chem. 29 (1990) 2855.
[48] B.P. Sullivan, D.J. Salmon, T.J. Meyer, Inorg. Chem. 17 (1978) 3334.
[49] E.J. Gabe, Y. Le Page, J.P. Charland, T.L. Lee, P.S. White, Appl. Cryst. 22 (1989) 384.
[50] G.M. Sheldrick, Acta Cryst. A46 (1990) 467.
[51] G.M. Sheldrick, SHELXL (1992), A Program for the refinement of crystal structures, University of Gottingen, Germany, Pre-release version.
[52] T. Matsubara, C. Creutz, Inorg. Chem. 18 (1979) 1956.
[53] H.C. Bajaj, R. Van Eldik, Inorg. Chem. 27 (1988) 4052.
[54] H.C. Bajaj, R. Van Eldik, Inorg. Chem. 28 (1989) 1980.
[55] A. Das, H.C. Bajaj, D. Chatterjee, Polyhedron 14 (1995) 3585.
[56] A. Das, H.C. Bajaj, Polyhedron 16 (1997) 1023.
[57] D. Chatterjee, H.C. Bajaj, A. Das, Inorg. Chim. Acta 24 (1994) 189.
[58] D. Chatterjee, H.C. Bajaj, A. Das, Inorg. Chem. 32 (1993) 4049.
[59] P.D. Beer, O. Kocian, R.J. Mortimer, J. Chem. Soc. Dalton Trans (1990) 3283.
[60] R.J. Shaw, R.T. Webb, I.R.H. Schmeh, J. Am. Chem. Soc. 112 (1990) 1117.
[61] C.K. Johnson (1965), ORTEP, Report ORNL-3794, Oak Ridge National Laboratory, TN.
[62] J.C. Chambron, C. Coudret, J.-P. Sauvage, New J. Chem. 16 (1992) 361.
[63] A. Das, J.C. Jeffery, J.P. Maher, J.A. McCleverty, E. Schatz, M.D. Ward, G. Wollermann, Inorg. Chem. 32 (1993) 2145.
[64] E.C. Constable, M.D. Ward, J. Chem. Soc. Dalton Trans (1990) 1450.
[65] M.J. Poweres, T.J. Meyer, J. Am. Chem. Soc. 102 (1980) 1289.
[66] C.A. Bignozi, S. Roffia, C. Chiorboli, J. Davila, M.T. Indelli, F. Scandola, Inorg. Chem. 28 (1989) 4350.
[67] S. Roffia, R. Casudei, F. Paolucci, C. Paradisi, C.A. Bignozi, F. Scandola, J. Electroanal. Chem. 302 (1991) 157.
[68] M.M. Taqui Khan R.M. Naik, Polyhedron 8 (1989) 463.
[69] Y.S. Sohn, D.A. Hendrickson, H.B. Gray, J. Am. Chem. Soc. 93 (1971) 3603.
[70] V. Balzani, F. Scandola, Supramolecular Photochemistry, Ellis Horwood, UK, 1991.
[71] K. Kalyanasundaram, Photochemistry of Polypyridyl, Porphyrin Complexes, Academic Press, London, 1992.
[72] J. Mcalvert, J.V. Caspar, R.A. Binstead, T.D. Westmoreland, T.J. Meyer, J. Am. Chem. Soc. 104 (1982) 6620.
[73] W.M. Wacholtz, R.A. Auerbach, R.H. Schenhl, M. Ollino, W.R. Cheroy, Inorg. Chem. 24 (1985) 1758.
[74] J.V. Caspar, T.J. Meyer, Inorg. Chem. 22 (1983) 2444.
[75] P.P. Zarnegar, C.R. Bock, D.G. Whitten, J. Am. Chem. Soc. 93 (1973) 4367.
[76] A. Juris, V. Balzani, F. Barigelletti, S. Campagna, P. Belser, A.V. Zelewsky, Coord. Chem. Rev. 84 (1988) 85 and Refs. therein.
[77] M.S. Wrighton, L. Pdungsap, D.L. Morse, J. Phys. Chem. 79 (1975) 66.
[78] G.L. Ganies, M.P. O'Neil, W.A. Svec, M.P. Niemczyk, M.R. Wasielewsky, J. Am. Chem. Soc. 113 (1991) 719.